

# Organometallic chemistry at the nanoscale. Dendrimers for redox processes and catalysis\*

Didier Astruc

*Laboratoire de Chimie Organique et Organométallique, UMR CNRS No 5802,  
Université Bordeaux I, 33405 Talence Cedex, France*

*Abstract:* An overview of the metal-mediated synthesis and use of nanosized metallodendrimers is given with emphasis on electron-transfer processes (molecular batteries consisting in dendrimers decorated with a large number of equivalent redox-active centers) and catalytic reactions (electron-transfer-chain catalytic synthesis of dendrimers decorated with ruthenium carbonyl clusters, redox catalysis of nitrate and nitrite electroreduction in water by star-shape hexanuclear catalysts).

## INTRODUCTION

Although most rules of stoichiometric and catalytic organometallic activation are now known [1], there remains a wide-open field of research for development and applications using the exploration of the best metal-ligand combination toward a given reaction. Present examples can now be found in metathesis that remained restricted to nonfunctional olefins for a long time until the recent successful efforts of Grubbs' [2] and Schrock's groups [3]. Their commercial catalysts are now of everyday use for organic and polymer chemists. A previous success story of this kind started in 1970 when Kagan first published efficient asymmetric catalysis with the powerful concept of chiral chelating phosphine [4]. This idea led many chemists, including other prestigious ones, to find optically active drugs with close to 100 % ee, an essential requirement for safe use by the public [5].

What now remains to be done? Indeed, the task is enormous for 21<sup>st</sup> century organometallic and molecular chemists. Mononuclear homogeneous catalysts [6] cannot be easily removed, thus they contaminate products and cannot be re-used. Heterogeneous catalysts often have poor selectivity, their mechanism of action is not well defined, and they also suffer from damage from one batch to the next [7]. Finally, supported catalysts do not always work as well or in the same fashion as homogeneous analogs, their distribution in the polymer is not well defined, they suffer from leaching, and by no means represent a definitive solution as witnessed by the poor extension to the industrial level [8]. An analogous reasoning can be made in other fields such as molecular electronics and sensors, in which the absence of impurities can be crucial. Organometallic chemistry is a fantastic tool to activate molecules, make bonds and introduce functions, but at the same time many challenges remain in order to fill the gaps toward applications.

Therefore, we have engaged in a large research program aimed at carrying organometallic chemistry at the nanoscale level. The goals are to design nanoscale organometallic catalysts, sensors, and components for molecular electronics that will not only be easily separated from other products, but whose molecular definition should be as precise as that of monometallic compounds and yet be addressable by macrocomponents such as monodisperse polymers, electrodes, and surfaces. In the present review, we provide a few examples in this direction. Dendrimers, a young field of molecular chemistry [8,9], are the first perfectly defined synthetic macromolecules (i.e., of polydispersity 1.0) that are

\*Plenary lecture presented at the XX<sup>th</sup> International Conference on Organometallic Chemistry (ICOMC), Corfu, Greece, 7–12 July 2002. Other presentations are published in this issue, pp. 421–494.

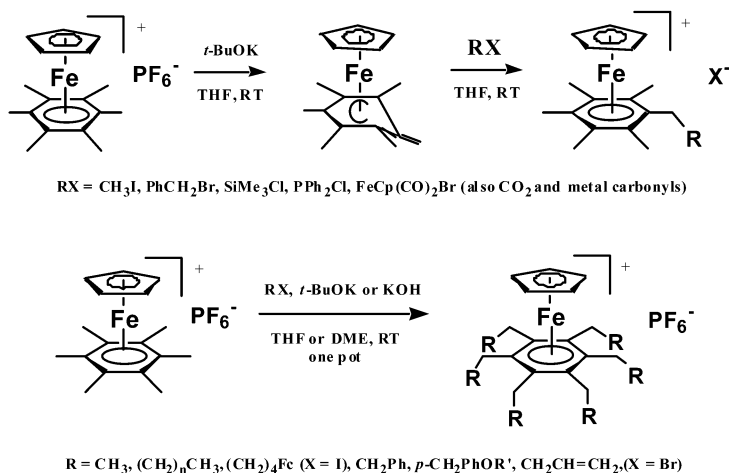
ideal for the precise loading of homogeneous catalysts [10], sensors, and devices for molecular electronics. We will show that the use of organo-iron chemistry allows the fast construction of dendritic cores, dendrons, and large dendrimers. Other nanoscale molecules of interest, such as organometallic ring systems, can also be made. Then, we will use the dendrimers to decorate them with metal-sandwich-type redox systems that provide a large number of electrons exchangeable at about the same redox potential. This property makes them actual candidates for molecular batteries. Then, we will give examples of the clean introduction of ruthenium clusters onto dendritic phosphines using electron-transfer-chain catalysis, and finally show how water-soluble organometallic dendritic catalysts can function without kinetic loss for redox-catalyzed reactions as compared to their monometallic analogs having the same driving force. The latter aspect leads us to think in terms of green chemistry, a parameter that will hopefully become more and more essential in the future. The part of our research devoted to sensors involving metallocendrimers [11,12], gold nanoparticles [13], and self-assembled monolayers on electrode surfaces [14] is more relevant to inorganic chemistry and will not be detailed here. The interested reader, however, may be referred to recent original publications in these areas [11–14].

## ORGANO-IRON SYNTHESES OF POLYALLYL DENDRITIC CORES, DENDRONS, AND LARGE DENDRIMERS

In the robust, easily accessible cationic complexes  $[\text{FeCp}(\text{arene})][\text{PF}_6]$ , the benzylic protons are more acidic than in the free arene because of the electron-withdrawing character of the 12-electron  $\text{CpFe}^+$  moiety. For instance,  $[\text{FeCp}(\text{C}_6\text{Me}_6)][\text{PF}_6]$  is more acidic by 15 pKa units (pKa = 28 in DMSO) than in the corresponding free arene (pKa = 43 in DMSO). As a result, these complexes are much more easily deprotonated than the free arene [15,16]. This key proton-reservoir property led us to synthesize stars and dendrimers in an easy way [15]. Indeed, reaction of  $[\text{FeCp}(\text{C}_6\text{Me}_6)][\text{PF}_6]$  [17–19], with excess KOH (or *t*-BuOK) in THF or DME and excess methyl iodide, alkyl iodide, allyl bromide, or benzyl-bromide result in the one-pot hexasubstitution (Scheme 1) [20–22]. With alkyl iodides, the reaction using *t*-BuOK only leads to dehalogenation of the alkyl iodide giving the terminal olefin. Thus, one must use KOH, and the reactions with various alkyl iodides (even long-chain ones) were shown to work very well with this reagent to give the hexaalkylated  $\text{Fe}^{II}$ -centered complexes. The hexaalkylation was also performed with alkyl iodides containing functional groups at the alkyl chain termini [23]. For instance, 1-ferrocenylbutyl iodide reacts nicely to give the hexaferrocene star containing the  $\text{CpFe}^+$  center [24]. The reaction with excess benzylbromide [20,24], *p*-alkoxybenzylbromide [24], or *p*-bromobenzylbromide [24] only gives the hexabenzylated, hexa-*p*-alkoxybenzylated, or hexa-*p*-bromobenzylated complex as the ultimate reaction product. Cleavage of the methyl group in the *p*-methoxybenzyl derivatives synthesized in this way yields the hexaphenolate stars that could be combined with halogen-containing organometallic compounds [24b,c].

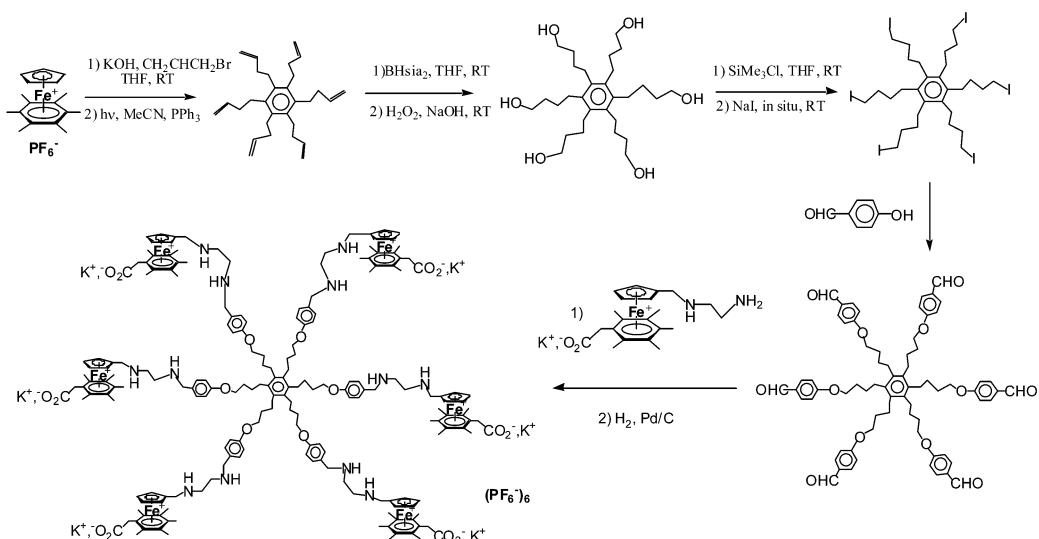
It is remarkable that the allyl group (as allyl bromide or iodide) is the only one leading to complete double branching of the  $\text{C}_6\text{Me}_6$  complex.  $\text{CpFe}^+$ -induced dodecaallylation of  $\text{C}_6\text{Me}_6$  indeed gives the extremely bulky dodecaallylation product [26] that can be reached when the reaction is prolonged for two weeks at 40 °C. The chains are blocked in a directionality that cannot convert into its enantiomer and makes the metal complex chiral. Both the hexa- and dodecaallylation reactions are well controlled.

Alkynyl halides cannot be used in the  $\text{CpFe}^+$ -induced hexafunctionalization reaction, but alkynyl substituents can be introduced from the hexaalkene derivative by bromination followed by dehydrohalogenation of the dodecabromo compound [27]. The hexaalkene is also an excellent starting point for further syntheses, especially using hydroelementation reactions. Hydrosilylation reactions catalyzed by Speir's reagent led to long-chain hexasilanes [28], and hydrometallations were also achieved using  $[\text{ZrCp}_2(\text{H})(\text{Cl})]$  [29]. The hexazirconium compound obtained is an intermediate for the synthesis of the hexa-iodo derivative [29]. One of the most useful hydroelementation reactions of the hexabutenyl derivatives is the hydroboration leading to the hexaborane. The latter is oxidized to the hexaoxide using  $\text{H}_2\text{O}_2$  under basic condition [21]. This chemistry can be carried out on the iron complex or alternatively on



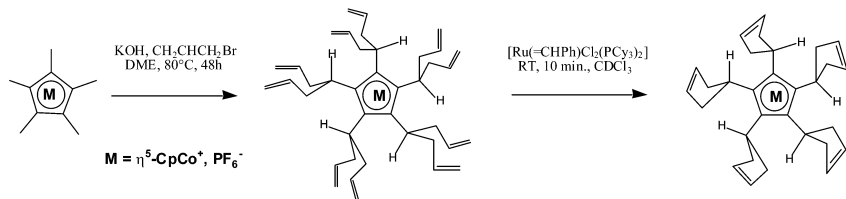
**Scheme 1** Deprotonation of  $[\text{FeCp}(\eta^6\text{-C}_6\text{Me}_6)]\text{[PF}_6^-$  followed by reactions with electrophiles (top) and one-pot hexafunctionalization of this complex under ambient conditions (bottom). The top reaction illustrates the mechanism of the bottom one.

the free hexaalkene which may be liberated from the metal by photolysis in  $\text{CH}_2\text{Cl}_2$  or MeCN using visible light [20]. The polyol stars and dendrimers can be transformed into mesylates and iodo derivatives that are useful for further functionalization. The hexaoil is indeed the best source of hexaiodo derivatives either using HI in acetic acid or even better by trimethylsilylation using  $\text{SiMe}_3\text{Cl}$  followed by iodination using  $\text{NaI}$  [30]. Williamson coupling reactions between the hexa-ol and 4-bromomethylpyridine or -polypyridine led to hexapyridine and hexapolypyridine and to their ruthenium complexes [31,32]. This hexaiodo star was condensed with *p*-hydroxybenzaldehyde to give a hexabenzaldehyde star, which could further react with substrates bearing a primary amino group. Indeed, this reaction yielded a water-soluble hexametallic redox catalysts, which was active in the electroreduction of nitrate and nitrite to ammonia in basic aqueous solution, *vide infra* (Scheme 2) [33–35].



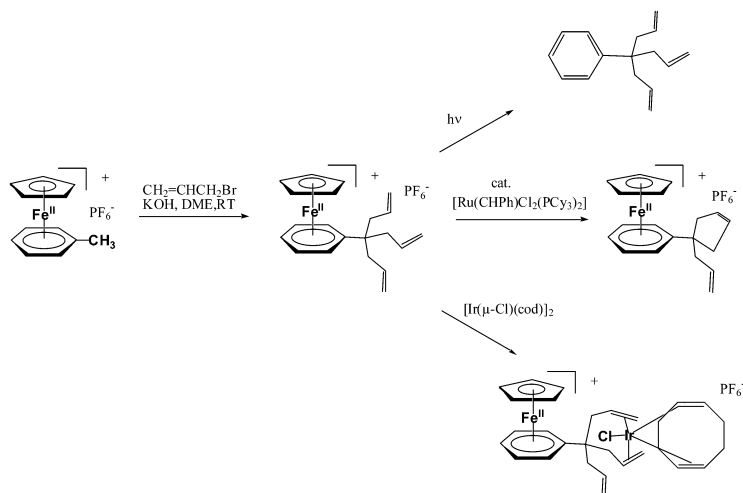
**Scheme 2**  $\text{CpFe}^+$ -induced hexaallylation of  $\text{C}_6\text{Me}_6$  and subsequent hexafunctionalization of the aromatic stars with the heterodifunctional, water-soluble organometallic redox catalyst (bottom) for the cathodic reduction of nitrates and nitrites to ammonia in water, see the section “Water-soluble dendritic organometallic redox catalysts”.

If the hexafunctionalization of hexamethylbenzene leads to stars, the octafunctionalization of durene leads to dendritic cores. The first of these octa-alkylation reactions was reported as early as 1982, and led to a primitive dendritic core containing a metal-sandwich unit [20]. Thus, as the hexafunctionalization, this reaction is very specific. Two hydrogen atoms of each methyl group are now replaced by two methyl, allyl, or benzyl groups [26]. Applications to the synthesis of dendrimers containing 8 [36] or 24 redox-active groups has recently been reported. Double branching, i.e., replacement of two out of three hydrogen atoms by two groups on each methyl substituent of an aromatic ligand coordinated to an activating cationic group  $\text{CpM}^+$  in an 18-electron complex, is also easily obtained in the pentamethylcyclopentadienyl ligand in pentamethyl cobaltocenium [37] and in penta- [38] and deca-methylrhodocenium [39]. The interconversion of the two directionalities of deafunctionalized ligands coordinated to  $\text{CpCo}^+$  or  $\text{CpRh}^+$ , which could be observed by  $^1\text{H}$  NMR for the deaisopropyl- and deaisopentyl cyclopentadienyl cobalt and rhodium complexes [37–39] (Scheme 3).



**Scheme 3** Decaallylation of 1,2,3,4,5-pentamethylcobaltocenium in a one-pot reaction consisting of 10 deprotonation-allylation sequences (steric constraints inhibit further reaction, and the 10 groups introduced are self-organized according to a single directionality) and follow-up RCM of the deafunctionalized complex.

In all the above examples, the polybranching reaction of arene ligands was limited by the steric bulk. In the toluene and mesitylene ligands, the deprotonation-allylation reactions are no longer restricted by the neighborhood of other alkyl groups. All the benzylic protons, i.e., three per benzylic carbon, can be replaced by methyl or allyl groups in the one-pot iterative methylation or allylation reactions [30]. Thus, the toluene complex can be triallylated, and the resulting tripod can be desymmetrized by stoichiometric [40] or catalytic reaction [41] with transition metals shown in Scheme 4. The metathesis reaction, in particular, is complete in 5 min at room temperature using the first-generation Grubbs'

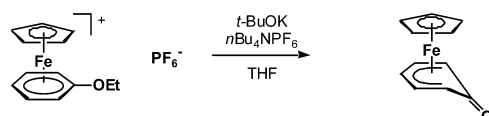


**Scheme 4** One-pot  $\text{CpFe}^+$ -induced triallylation of toluene and reactions of transition-metal complexes with the triallylated complex.

catalyst  $[\text{Ru}(\text{=CHPh})\text{Cl}_2(\text{PCy}_2)_2]$  [2] with many polyallylated complexes  $[\text{FeCp}(\text{arene})]^+$  described above, as well as to the decaallylated cobalt complex [41]. The reaction is very selective, and terminal double bonds remain unreacted using this catalyst at room temperature.

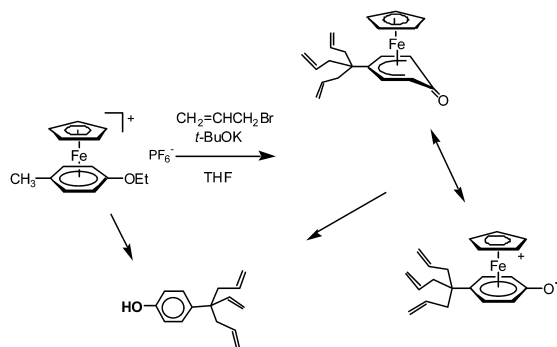
The mesitylene complex can be nonaallylated, these reactions being carried out smoothly at room temperature in the presence of excess KOH and allyl bromide. The nonaallyl complex was photolyzed using visible light to remove the metal group  $\text{CpFe}^+$ , then hydroborated using 9-BBN, and the nonaborane was oxidized using  $\text{H}_2\text{O}_2/\text{OH}^-$  to the nona-ol [30].

The triple branching reaction of Scheme 4 being very straightforward, we sought a more sophisticated version compatible with a functional group in the para position of the tripod in order to open the access to a functional dendron. Serendipitously, we found that KOH or *t*-BuOK easily cleaved the iron complexes of aromatic ethers under very mild conditions. The activating  $\text{CpFe}^+$  group again induces this reaction, which is very general for a variety of aromatic ether complexes (Scheme 5) [42,43].



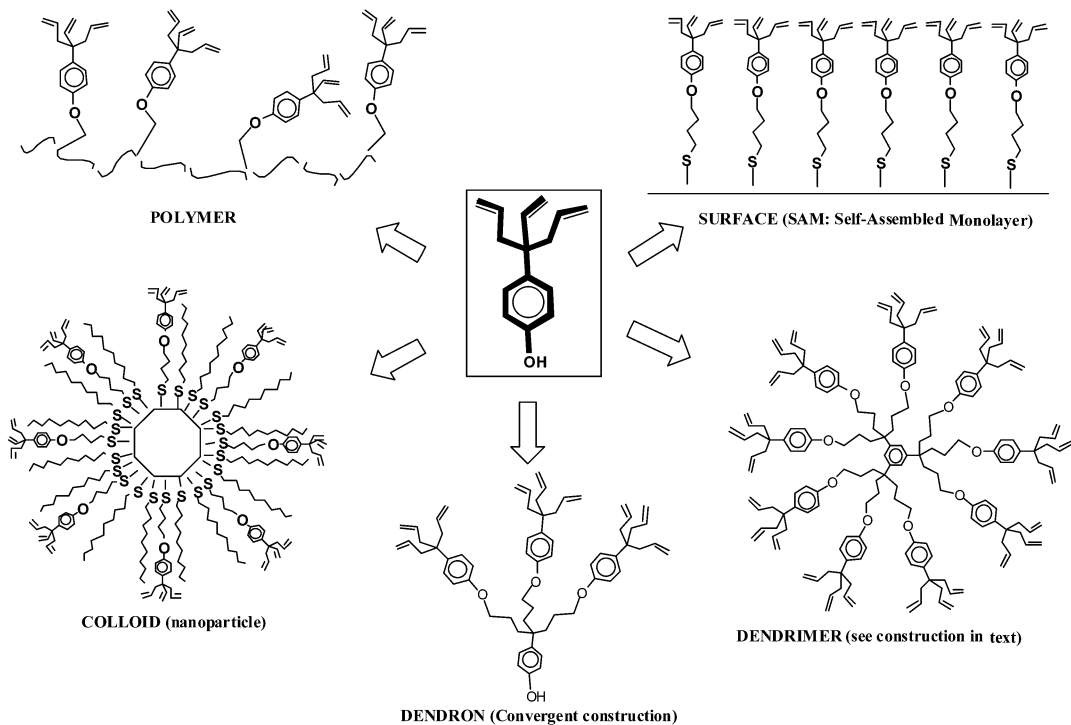
**Scheme 5** Heterolytic C–O cleavage reaction in aryl ether complexes by *t*-BuOK or KOH induced by the activating 12-electron fragments  $\text{CpFe}^+$ .

Since this cleavage reaction is carried out with the same reagent and solvent as the one used in the trialkylation reaction (ideally, *t*-BuOK in THF), we have attempted to perform both reactions in a well-defined order (trialkylation before ether cleavage) in a one-pot reaction. Indeed, this works out well, and the  $\text{CpFe}^{\text{II}}$  complex of the phenol tripod was made in 50 % yield in this way. This complex can be photolyzed in the usual way using visible light, which yields the free phenol tripod. However, we have also further investigated the possibility of obtaining the cleavage of the arene ligand in situ at the end of the phenol tripod construction; *t*-BuOK is a reductant when it cannot perform other reactions. Since the two important reactions are over, then comes the third role of *t*-BuOK: single-electron reductant. Reasoning in this way turned out to be correct. The cleavage of the arene intervenes rapidly at the 19-electron stage because 19-electron complexes of this kind are not stable with a heteroatom located in the exocyclic position (most probably because the heteroatom coordinates to the metal from the labile 19-electron structure). After optimizing the reaction conditions, a 50 % yield of free phenol dendron from the ethoxytoluene complex could be reproducibly obtained [44,45], and this reaction is now currently used in our laboratory to synthesize this very useful dendron as a starting material (Scheme 6).

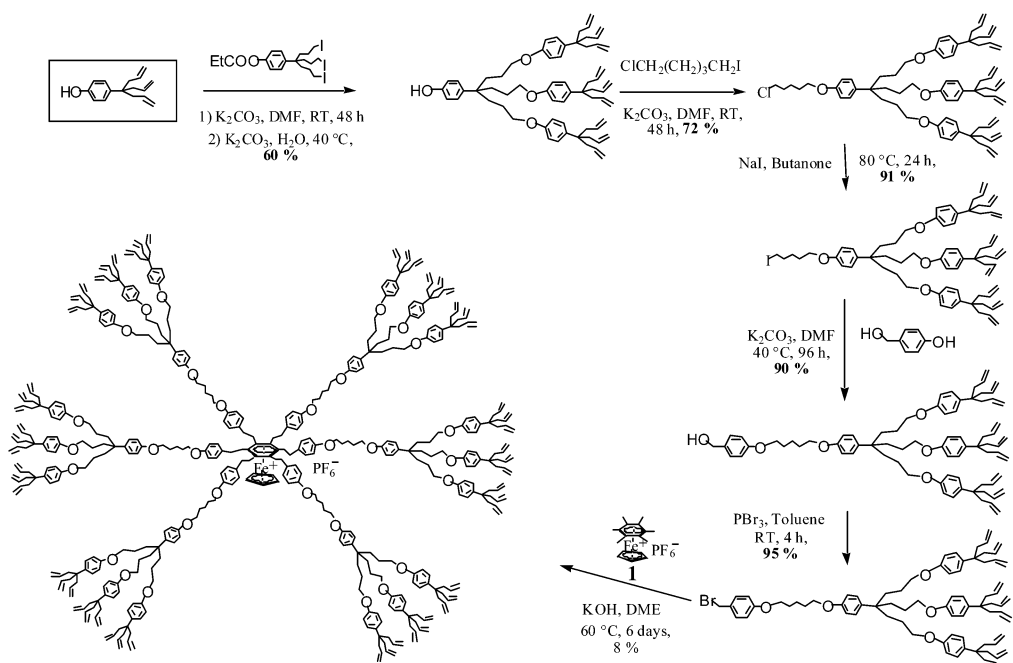


**Scheme 6** One-pot syntheses of the phenoltriallyl iron complex and metal-free dendron by variation of the experimental conditions.

This phenoltriallyl dendron has been functionalized at both the phenolic and allylic positions. For instance, the dendron can be bound, after suitable molecular engineering, to the branches of a phenolic-protected dendron (convergent construction) onto stars, and dendritic cores (divergent construction), nanoparticles, surfaces, and polymers (Scheme 7). An example is provided by the  $\text{CpFe}^+$ -induced hexafunctionalization by a phenol-nonaallyl dendron (prepared according to such a convergent synthesis) that was functionalized in phenolic position by a tail terminated by a benzylbromide group. This type of strategy allows direct access to large dendrimers by simply using the  $\text{CpFe}^+$ -induced hexafunctionalization reaction that gives hexa-branch stars with linear organic halides (Scheme 8).



**Scheme 7** Example of the linkage of the phenoltriallyl dendron to various nanostructures.

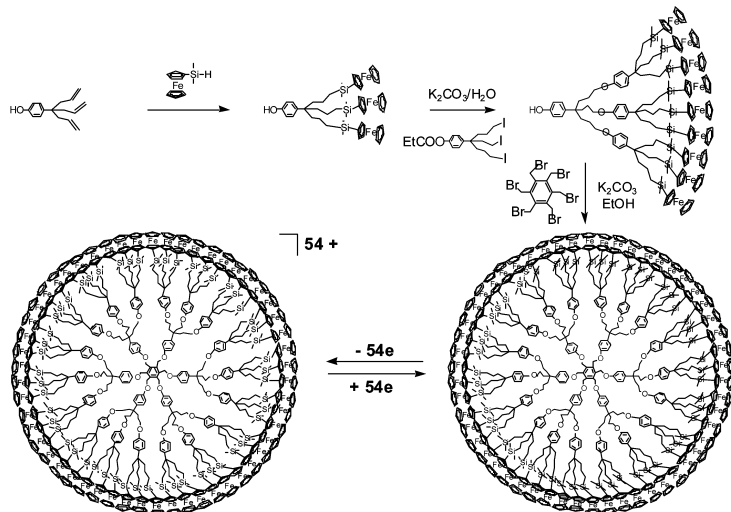


**Scheme 8**  $\text{CpFe}^+$ -induced hexabenzylation of  $\text{C}_6\text{Me}_6$  applied to direct convergent dendrimer synthesis of a 54-allyl dendrimer.

## DECORATION OF DENDRIMERS WITH REDOX-ACTIVE GROUPS: TOWARD MOLECULAR BATTERIES

The functionalization of the three allyl chains of the phenol dendron could be achieved by hydrosilylation reaction catalyzed by the Karsted catalyst [46]. Indeed, it is very interesting that there is no need to protect the phenol group before performing these reactions. For instance, catalyzed hydrosilylation using ferrocenyldimethylsilane gives a high yield of the triferrrocenyl dendron  $\text{HO}^\bullet\text{C}_6\text{H}_4\text{C}(\text{CH}_2\text{CH}_2\text{CH}_2\text{SiMe}_2\text{Fc})_3$  that is easily purified by column chromatography [46,47]. Protection of the phenol dendron using propionyliodide gave the phenolate ester, which was hydroborated. Oxidation of the triborane using  $\text{H}_2\text{O}_2/\text{OH}^-$  gave the triol, then reaction with  $\text{SiMe}_3\text{Cl}$  gave the tris(silyl) derivative. Reaction with  $\text{NaI}$  yielded the tri-iodo compound, and reaction with the tri-ferrocenyl dendron provided the nonaferrocenyl dendron that was deprotected using  $\text{K}_2\text{CO}_3$  in DMF. The nonaferrocenyl dendron was allowed to react with hexakis(bromomethyl)benzene, which gave the 54-ferrocenyl dendrimer. This convergent synthesis is clean, and the 54-ferrocenyl dendrimer gave correct analytical data (Scheme 9).

This approach is somewhat limited, however, since larger dendrons, which one would like to synthesize in this way, cannot be made because dehydrohalogenation becomes faster than nucleophilic substitution of the iodo by phenolate for bulkier higher generations of dendrons. Although this problem might be overcome by modifying the iodo branch in such a way that there would be no hydrogens in  $\beta$  positions, the condensation of higher dendrons onto a core would become tedious or impossible for steric reasons. This well-known inconvenience is intrinsic to the convergent dendritic synthesis. On the other hand, divergent syntheses are not marred by such a problem since additional generations and terminal groups are added at the periphery of the dendrimer. The limit is indicated by De Gennes, i.e., the steric congestion encountered at a generation where the peripheral branches can no longer be divided. Another obvious limit intervenes if the molecular objects added onto the termini of the branches are



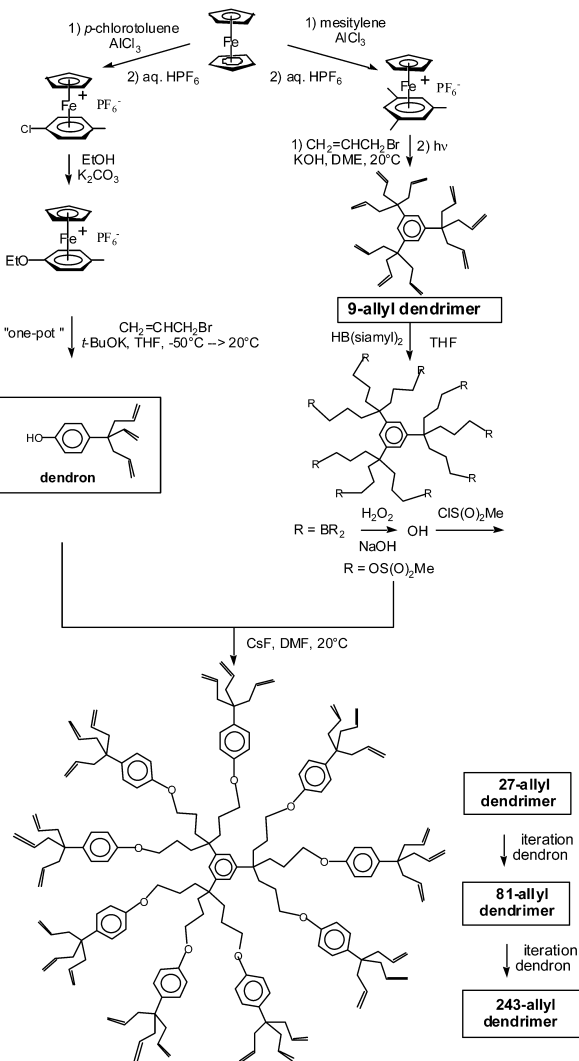
**Scheme 9** Convergent synthesis of a redox-robust 54-silylferrocenyl dendrimer.

large and interfere with one another. We have developed a divergent synthesis of polyallyl dendrimers indicated on Scheme 10 whereby each generation consists in hydroboration, oxidation of the borane to the alcohol, formation of the mesylate, and reaction of the phenol dendron with the mesylate. This strategy has allowed us to synthesize dendrimers of generation 0, 1, 2, and 3 with respectively 9 ( $G_0$ ), 27 ( $G_1$ ), 81 ( $G_2$ ), and 243 branches ( $G_3$ ) (Fig. 1).

The MALDI TOF mass spectrum of the 27-allyl dendrimer only shows the molecular peak with only traces of side product. That of the 81-allyl shows a dominant molecular peak, but also important side products resulting from incomplete branching. That of the 243-allyl could not be obtained, possibly signifying that this dendrimer is polydisperse (correct  $^1\text{H}$  and  $^{13}\text{C}$  NMR spectra were obtained, however, indicating that the ultimate reactions had proceeded to completion). This dendrimer was soluble, which indicated that this generation is not the last one, which might be reached. Larger dendrimers have recently been synthesized using a slightly different strategy. The ferrocenylsilylation of all these polyallyl dendrimers was carried out using ferrocenyldimethylsilane in ether or toluene and was catalyzed by the Karsted catalyst [48,49] at 40–45 °C (Scheme 11). The reactions were complete after two or three days except for the ferrocenylsilylation of 243-allyl that required a reaction time of one week, indicating some degree of steric congestion.

The  $^1\text{H}$  and  $^{13}\text{C}$  spectra indicated the absence of regioisomer. The solubility in pentane decreased from good for the 9-Fc dendrimer to low for the 27-Fc dendrimer and nil for the higher dendrimers, but the solubility in ether remained good for all the ferrocenyl dendrimers. Likewise, the retention times on plate or column chromatography increased with generation, and no migration was observed for the “243-Fc” dendrimer. The silane used here,  $\text{HSi}(\text{Fc})\text{Me}_2\text{Cl}$ , reported by Pannel and Sharma [50], was already used by Jutzi [51] to synthesize the decaferrocenyl dendrimer [ $\text{Fe}(\text{CCH}_2\text{CH}_2\text{SiMe}_2\text{Fc})_{10}$ ] (with Fc = ferrocenyl) from decaallylferrocene.

The cyclic voltammetry of all the ferrocenyl dendrimers on Pt anode shows that all the ferrocenyl centers are equivalent, and only one wave was observed. It was possible to avoid adsorption using even  $\text{CH}_2\text{Cl}_2$  for the small ferrocenyl dendrimers, but it was required to use MeCN for the medium-sized ones (27-Fc, 54-Fc, and 81-Fc). Finally, adsorption was not avoided even with MeCN for the “243-Fc” dendrimer. From the intensity of the wave, the number of ferrocenyl units could be estimated using the Anson–Bard equation [52], and the number found was within 5 % of the branch numbers except for the “243-Fc” dendrimer, for which the experimental number was too high (250) because of the adsorption.



**Scheme 10** Strategy for the construction of large dendrimers starting from ferrocene.

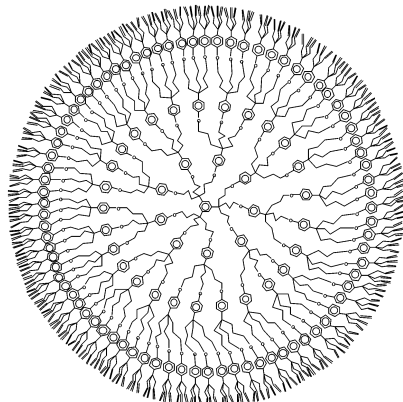
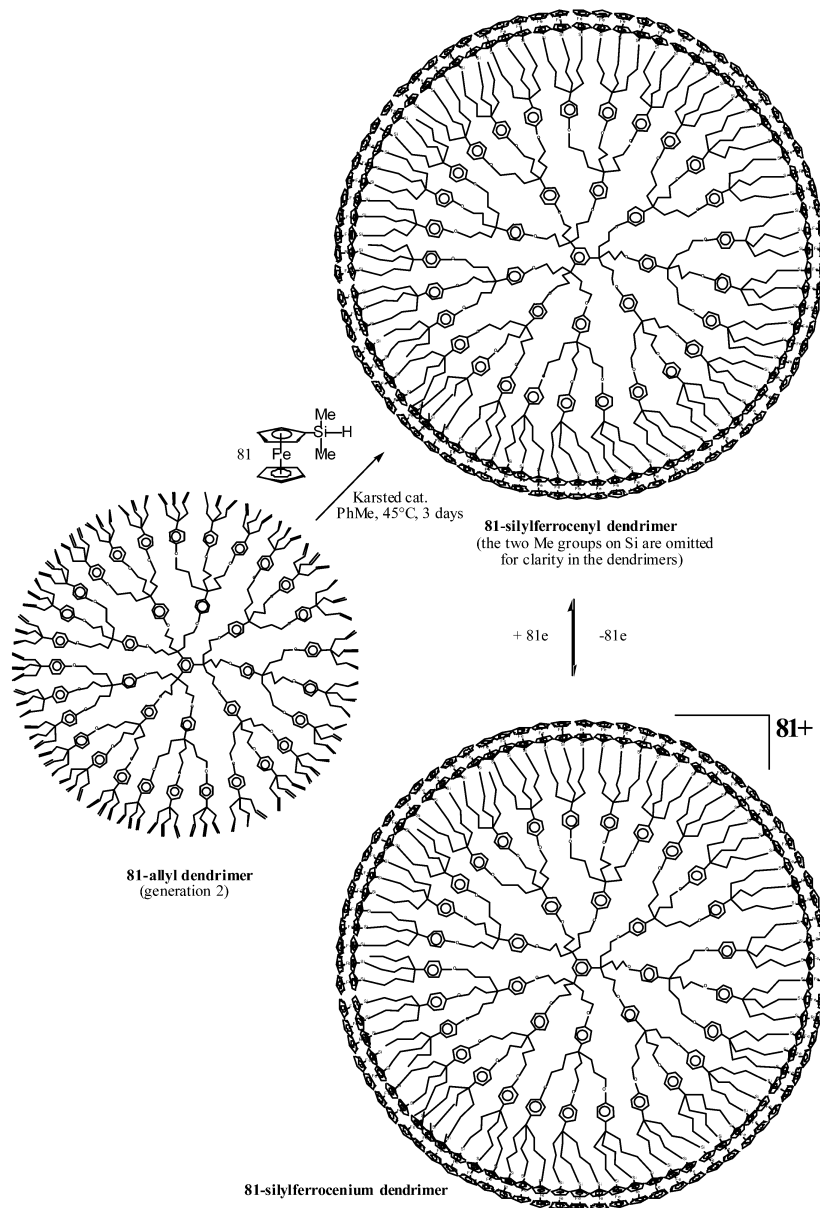


**Fig. 1** 243-allyl dendrimer (3<sup>rd</sup> generations; see the constructions on Scheme 10).



**Scheme 11** Ferrocenylsilylation of the polyallyl dendrimers synthesized. Example of the 2<sup>nd</sup> generation 81-allyl dendrimer.

The first polyferrocenium dendrimers reported by our group in 1994 and characterized inter alia by Mössbauer spectroscopy (a “quantitative” technique) were mixed-valence Fe<sup>II</sup>/Fe<sup>III</sup> complexes [23]. Since then, we have been seeking to synthesize larger ferrocenyldendrimers, which could also withstand oxidation to their ferrocenium analogs. The syntheses of amidoferrocene dendrimers were reported five years ago simultaneously by our group [11,53] and the Madrid group using different cores [54,55]. In our reports, we were able to show the use of these metallocendrimers as redox sensors for the recognition of oxo-anions, with remarkable positive dendritic effects when the generation increased. The amidoferrocenyl dendrimers are not the best candidates for a stable redox activity on the synthetic scale,

however, and thus even less so for molecular batteries. Indeed, although they give fully reversible cyclic voltammetry waves, it is known that ferrocenium derivatives bearing an electron-withdrawing substituent are at least fragile, if stable at all. This inconvenience is probably enhanced in the dendritic structures because of the steric effect that forces ferrocenium groups to encounter one another more easily than as monomers. Thus, we have oxidized our silylferrocenyl dendrimers using  $[NO][PF_6]$  in  $CH_2Cl_2$  and obtained stable polyferrocenium dendrimers as dark-blue precipitates, as expected from the known characteristic color of ferrocenium itself. These polyferrocenium dendrimers were reduced back to soluble orange polyferrocenyl dendrimers using decamethylferrocene as the reductant [56]. No decomposition was observed either in the oxidation or in the reduction reactions, which were very clean, and this redox cycle could be achieved in quantitative yield even with the “243-ferrocenyl” dendrimer. The zero-field Mössbauer spectrum of the 243-ferrocenium dendrimer showed a single line corresponding to the expected spectrum known for ferrocenium itself [57], confirming its electronic structure. Thus, these polyferrocenyl dendrimers are molecular batteries, which could be used in specific devices. Indeed, as large as they may be, they transfer a very large number of electrons rapidly and “simultaneously” with the electrode. By “simultaneously”, we mean that, visually, the cyclic voltammogram looks as if it were that of a monoelectronic wave. One must question the notion of the isopotential for the many ferrocenyl units at the periphery of a dendrimer. In theory, all the standard potentials of the  $n$  ferrocenyl units of a single dendrimer are distinct even if all of them are equivalent and independent. This situation arises because the charge of the overall dendrimer molecule increases by one unit of charge every time one of its ferrocenyl units is oxidized to ferrocenium. The next single-electron oxidation is more difficult than the preceding one because, the dendritic molecule having one more unit of positive charge, it is more difficult to oxidize because of the increased electrostatic factor. Thus, the potentials of the  $n$  redox units are statistically distributed around an average standard potential centered at the average potential (Gaussian distribution) [52]. In practice, the situation is complicated by the fact that the dendritic molecule, as large as it may be, is rotating much more rapidly than the usual electrochemical time scales [58,59]. Under these conditions, all the potentials are probably averaged. The fast rotation is also responsible for the fact that all the ferrocenyl units come close to the electrode within the electrochemical time scale. Consequently, there is no slowing down of the electron transfer due to the long distance from the electrode even in large dendrimers. Indeed, the waves of the ferrocenyl dendrimers always appear fully electrochemically reversible, indicating fast electron transfer.

The ferrocenyl dendrimers also adsorb readily on electrodes, a phenomenon already well known with various kinds of polymers [60]. When polymers contain redox centers, the adsorbed polymer have long been shown to disclose a redox wave for which the cathodic and anodic waves are located at exactly the same potential and the intensity of each wave is proportional to scan rate. Continuous cycling shows the stability of the adsorption of the electrode modified in this way. The ferrocenyl dendrimers described show this phenomenon as expected. The stability of the electrode modified by soaking the Pt electrode in a  $CH_2Cl_2$  solution containing the ferrocenyl dendrimer and cyclic scanning between the ferrocenyl and ferrocenium regions is all the better as the ferrocenyl dendrimer is larger. For instance, in the case of the 9-ferrocenyl dendrimer, scanning 20 times is necessary before obtaining a constant intensity, and this intensity is weak. With the 27-, 54-, 81-, and 243-ferrocenyl dendrimers, only approximately 10 cyclic scans are necessary before obtaining a constant wave, and the intensity is much larger. When such derivatized electrodes are washed with  $CH_2Cl_2$  and re-used with a fresh, dendrimer-free  $CH_2Cl_2$  solution, the cyclic voltammogram is obtained with  $\Delta E_p = 0$ . Other characteristic features are the linear relationship between the intensity and scan rate and the constant stability after cycling many times with no sign of diminished intensity (Fig. 2).

Under these conditions, one may note that the argument of the fast rotation of the dendritic molecule to bring all the redox centers in turn close to the electrode does not hold for modified electrodes. Some redox centers must be close to the electrode, and some must be far. It is probable that a hoping mechanism in the solid state is responsible for fast electron transfer and for averaging all the potentials of the different ferrocenyl groups of a single dendritic molecule around a mean value. The proximity of

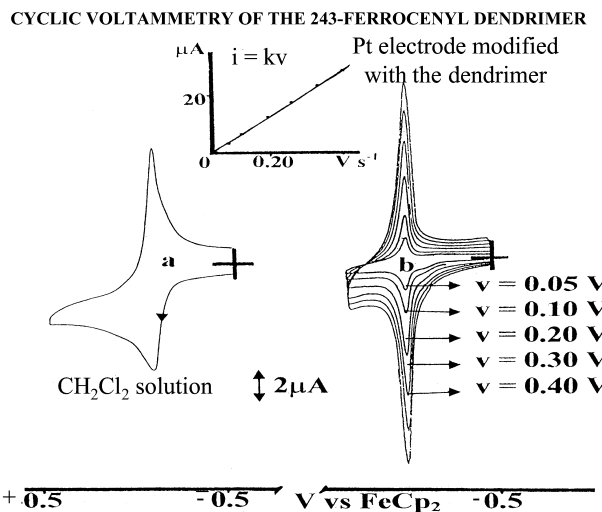
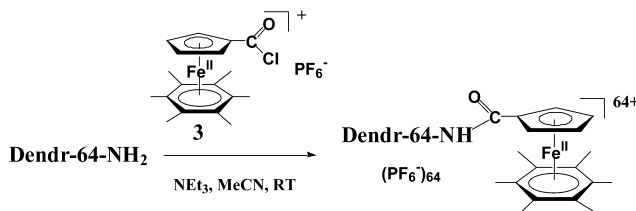


**Fig. 2** Cyclic voltammogram of the 243-ferrocenyl dendrimer ("243-Fc") in  $\text{CH}_2\text{Cl}_2$  solution containing  $0.1 \text{ M} [n\text{-Bu}_4\text{N}][\text{PF}_6]$ : (a) in solution ( $10^{-4} \text{ M}$ ) at  $100 \text{ mV s}^{-1}$  on Pt anode; (b) Pt anode modified with "243-Fc" at various scan rates, dendrimer-free clear  $\text{CH}_2\text{Cl}_2$  solution (inset: intensity as a function of scan rate: the linearity shows the expected behavior of a modified electrode with a fully adsorbed dendrimer).

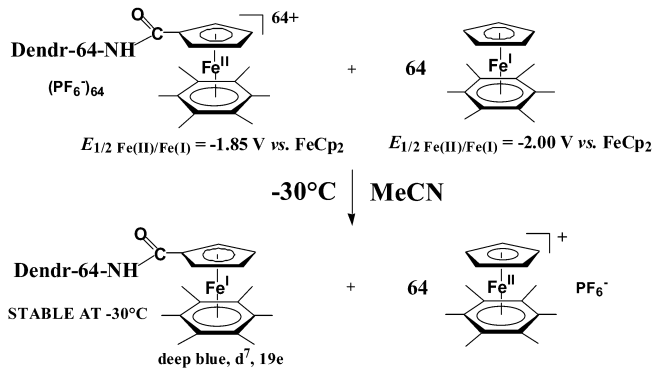
the ferrocenyl groups at the periphery of the dendrimer is a key factor, allowing this hoping to occur since it is known that electron transfer with redox sites, which are remote or buried inside a molecular framework, is slow, if at all observable [61–67].

Ferrocenes and ferrocenyl dendrimers are poor reductants. On the other hand, the complexes  $[\text{Fe}(\eta^5\text{-C}_5\text{R}_5)(\eta^6\text{-C}_6\text{Me}_6)]^{2+/+0}$  ( $\text{R} = \text{H}$  or  $\text{Me}$ ) have been shown to be efficient for various stoichiometric and catalytic electron-transfer reactions [16,68]. The covalent linkage of this sandwich complex to the  $\text{Cp}$  ligand by means of a chlorocarbonyl substituent leads, upon reaction with dendritic polyamines, to soluble  $\text{Fe}^{\text{II}}$  metallocendrimers. Moreover, these  $\text{Fe}^{\text{II}}$  metallocendrimers can be reduced to  $\text{Fe}^{\text{I}}$  by  $[\text{Fe}^{\text{I}}\text{Cp}(\eta^6\text{-C}_6\text{Me}_6)]$ , 1. Reduction of the monomeric model  $[\text{Fe}^{\text{II}}(\eta^5\text{-C}_5\text{H}_4\text{CONH}-n\text{-Pr})(\eta^6\text{-C}_6\text{Me}_6)][\text{PF}_6]$  by  $\text{Na}/\text{Hg}$  in THF (RT) gives the deep-blue-green, thermally stable 19-electron complex  $[\text{Fe}^{\text{I}}(\eta^5\text{-C}_5\text{H}_4\text{CONH}-n\text{-Pr})(\eta^6\text{-C}_6\text{Me}_6)]$  that shows the classic rhombic distortion of the  $\text{Fe}^{\text{I}}$  sandwich family, observable by electron paramagnetic resonance (EPR) in frozen THF at 77 K (3 g values around 2) [69]. Given this stability, we carried out the same reaction of  $[\text{Fe}^{\text{II}}(\eta^5\text{-C}_5\text{H}_4\text{COCl})(\eta^6\text{-C}_6\text{Me}_6)][\text{PF}_6]$  with the commercial polypropyleneimine dendrimer of generation 5 (64 amino termini) in  $\text{MeCN}/\text{CH}_2\text{Cl}_2$ : 2/1 in the presence of  $\text{NEt}_3$ . The polycationic metallocendrimer DAB *dendr*-64— $\text{NHCOCPFe}^{\text{II}}(\eta^6\text{-C}_6\text{Me}_6)$ , was obtained as the  $\text{PF}_6^-$  salt, soluble in  $\text{MeCN}$  and  $\text{DMF}$  (Scheme 12).

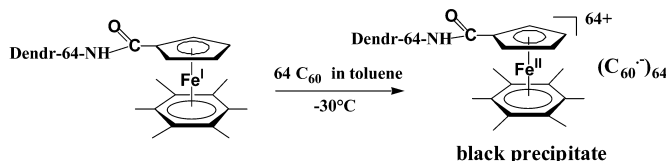


**Scheme 12** Covalent linkage of the complex  $[\text{FeCpCOCl}(\eta^6\text{-C}_6\text{Me}_6)][\text{PF}_6]$  to the DSM polyamine dendrimer of generation 5 (64 branches). Example of the 64-NH<sub>2</sub> dendrimer (generation 5).

This dendritic complex was characterized by  $^1\text{H}$  and  $^{13}\text{C}$  NMR and IR spectroscopies and cyclovoltammetry (a single reversible wave in DMF, at  $E_{1/2} = -1.84 \text{ V}$  vs.  $\text{FeCp}_2^{0+/+}$ ;  $\Delta E = 70 \text{ mV}$ ). Attempts to reduce it with the classic reductants that reduce monomeric complexes  $[\text{Fe}^{\text{II}}(\eta^5\text{-Cp})(\eta^6\text{-arene})][\text{PF}_6^-]$  such as Na sand, Na/Hg or  $\text{LiAlH}_4$  in THF or DME failed due to the insolubility of both the metallocendrimer and the reductant in the required solvents. The only successful reductant was the parent 19-electron complex  $[\text{Fe}^{\text{I}}\text{Cp}(\eta^6\text{-C}_6\text{Me}_6)]$  [70,71] (in pentane or THF) that reduced the metallocendrimer in MeCN at  $-30^\circ\text{C}$  to the neutral, deep-green-blue 19-electron  $\text{Fe}^{\text{I}}$  dendrimer in a few minutes (Scheme 13) [72].



**Scheme 13** Exergonic reduction of the cationic  $\text{Fe}^{\text{II}}$  dendritic sandwich groups by the parent 19-electron complex  $[\text{Fe}^{\text{I}}\text{Cp}(\eta^6\text{-C}_6\text{Me}_6)]$  to the  $\text{Fe}^{\text{I}}$  dendrimer complex. The exoergonicity of this electron-transfer reaction is  $0.16 \text{ V}$ , which is due to the electron-withdrawing effect of the juxta-cyclic carbonyl group on the Cp ring that lowers the reduction potential of the metallocendrimer as compared to that  $[\text{Fe}^{\text{I}}\text{Cp}(\eta^6\text{-C}_6\text{Me}_6)]$ . Although the  $\text{Fe}^{\text{I}}$  dendrimer decomposes at  $0^\circ\text{C}$ , it was also characterized by its EPR spectrum at  $10 \text{ K}$ , confirming, as the deep-blue-green color, the  $\text{Fe}^{\text{I}}$ -sandwich structure analogous to that of the monomeric model (Scheme 14).



**Scheme 14** Exergonic single-electron reduction of  $\text{C}_{60}$  by the dendritic  $\text{Fe}^{\text{I}}$  electron-reservoir complex.

Contrary to the case of  $[\text{Fe}^{\text{I}}\text{Cp}(\eta^6\text{-C}_6\text{Me}_6)]$  [69], however, it was not possible to record the EPR spectrum of the solution of the  $\text{Fe}^{\text{I}}$  dendrimer above  $10 \text{ K}$ . This is presumably due to the intramolecular relaxation among the peripheral  $\text{Fe}^{\text{I}}$  sandwich units. The intermolecular version of this relaxation effect is known to preclude observation of the spectrum of monomeric  $\text{Fe}^{\text{I}}$  sandwich complexes in the solid state above  $4 \text{ K}$  and in solution above  $77 \text{ K}$  [69]. This acetonitrile solution of the 64- $\text{Fe}^{\text{I}}$  dendrimer was used for the reaction with  $\text{C}_{60}$ , the stoichiometry being  $\text{Fe}^{\text{I}}/\text{C}_{60}$ :  $1/1$  ( $64 \text{ C}_{60}$  per dendrimer). Upon reaction with a toluene solution of  $\text{C}_{60}$ , the deep-blue-green color of the  $\text{Fe}^{\text{I}}$  dendrimer disappeared, leaving a yellow solution that contained  $[\text{Fe}^{\text{II}}\text{Cp}(\eta^6\text{-C}_6\text{Me}_6)][\text{PF}_6^-]$  and a black precipitate. Tentative extraction of this precipitate with toluene yielded a colorless solution, which indicated that no  $\text{C}_{60}$  was present. The Mössbauer spectra of this black solid at  $298 \text{ K}$  discloses parameters that show the presence of an  $\text{Fe}^{\text{II}}$  sandwich complex of the same family as  $[\text{Fe}^{\text{II}}\text{Cp}(\eta^6\text{-C}_6\text{Me}_6)]^+$  [69–71]. Its EPR spectrum recorded at  $77 \text{ K}$  shows the same EPR spectrum as that of  $[\text{Fe}^{\text{II}}\text{Cp}(\eta^6\text{-C}_6\text{Me}_6)]^+ \text{C}_{60}^-$  [73]. It could thus be concluded that  $\text{C}_{60}$  had been reduced to its monoanion, as designed for a process that is exergonic

by 0.9 V [74]. The  $[\text{dendr-Fe}^{\text{II}}]^+ \text{C}_{60}^-$  units being very large, they must be located at the dendrimer periphery, presumably with rather tight ion pairs, although the number of fullerene layers and overall molecular size are unknown (Fig. 3).

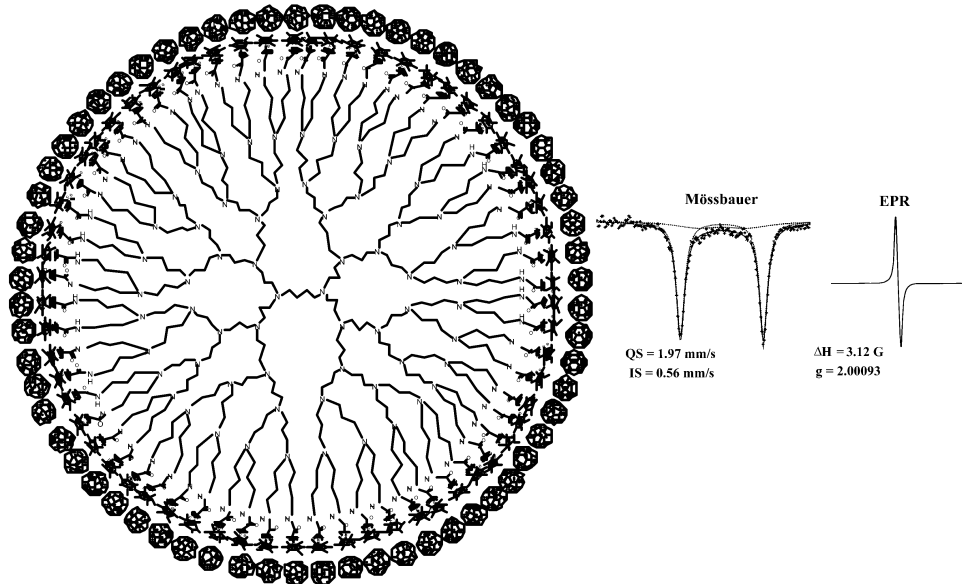
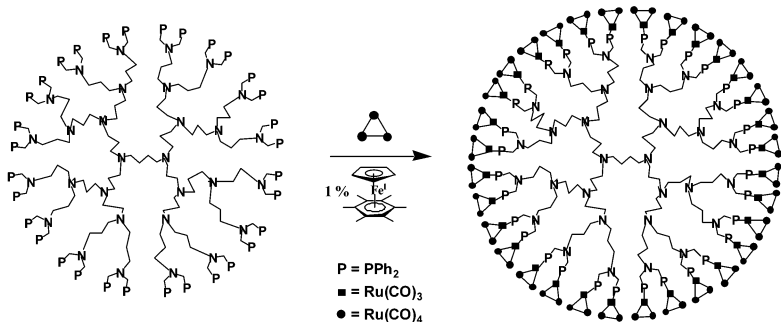


**Fig. 3** Dendr-64-NHCOCpFe( $\text{C}_6\text{Me}_6$ )<sup>64+</sup>, 64  $\text{C}_{60}^-$  resulting from the reaction of the 64-Fe<sup>I</sup> dendrimer with  $\text{C}_{60}$  in MeCN/toluene at -30 °C yielding the 64-Fe<sup>II</sup>- $\text{C}_{60}^-$  dendrimer with EPR spectrum (bottom, right) in MeCN at 10 K and Mössbauer spectrum at 77 K (bottom, left) of the latter.

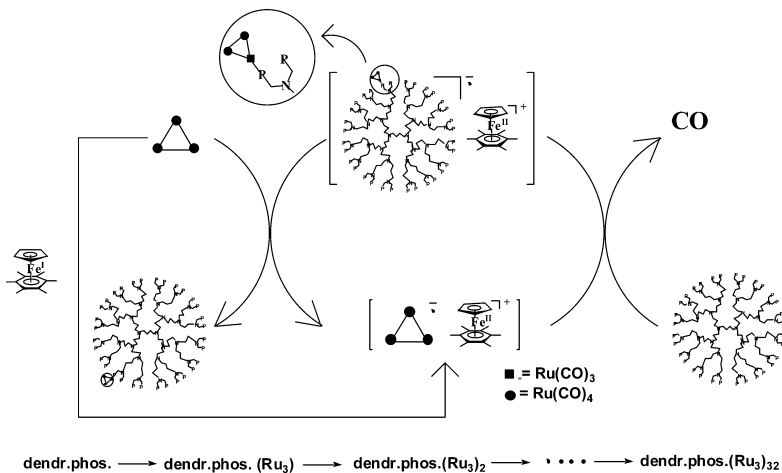
## DECORATION OF DENDRIMERS WITH RUTHENIUM CLUSTERS: TOWARD DENDRITIC CATALYSTS

The clean introduction of clusters onto the termini of polyphosphine dendrimers is a real challenge because of the current interest of dendritic clusters in catalysis and the mixtures usually obtained in thermal reactions of  $[\text{Ru}_3(\text{CO})_{12}]$  with phosphines. The diphosphine  $\text{CH}_3(\text{CH}_2)_2\text{N}(\text{CH}_2\text{PPh}_2)_2$  (abbreviated P-P below) was used as a simple, model ligand. The reaction between P-P and  $[\text{Ru}_3(\text{CO})_{12}]$  [75] (molar ratio: 1/1.05) in the presence of 0.1 equiv  $[\text{Fe}^{\text{I}}\text{Cp}(\eta^6\text{-C}_6\text{Me}_6)]$  in THF at 20 °C led to the complete disappearance of  $[\text{Ru}_3(\text{CO})_{12}]$  in a few minutes and the appearance of a mixture of chelate  $\{\text{P-P Ru}_3(\text{CO})_{10}\}$ , monodentate  $\{\text{P-P Ru}_3(\text{CO})_{11}\}$  and bis-cluster  $\{\text{P-P}[\text{Ru}_3(\text{CO})_{11}]_2\}$ . These reactions were reported by Bruce with simple diphosphines [76]. On the other hand, the reaction of P-P with  $[\text{Ru}_3(\text{CO})_{12}]$  in excess (1/4) and only 0.01 equiv  $[\text{Fe}^{\text{I}}\text{Cp}(\eta^6\text{-C}_6\text{Me}_6)]$  in THF at 20 °C led, in 20 min, to the formation of the air-stable, light-sensitive bis-cluster  $\{\text{P-P}[\text{Ru}_3(\text{CO})_{11}]_2\}$  as the only reaction product. Given the simplicity of the above characterization of the reaction product by  $^{31}\text{P}$  NMR and the excellent selectivity of this model reaction when excess  $[\text{Ru}_3(\text{CO})_{12}]$  was used, the same reaction between Reetz's dendritic phosphines [77a], derived from DSM's dendritic amines [77b], and  $[\text{Ru}_3(\text{CO})_{12}]$  could be more confidently envisaged. This reaction, catalyzed by 1 % equiv  $[\text{Fe}^{\text{I}}\text{Cp}(\eta^6\text{-C}_6\text{Me}_6)]$  was carried out in THF at 20 °C. The dendrimer-cluster assembly was obtained in 50 % yield. This shows the selectivity and completion of the coordination of each of the 32 phosphino ligands of P-P to a  $\text{Ru}_3(\text{CO})_{11}$  cluster fragment (Scheme 15).



**Scheme 15** Electron-transfer-chain catalyzed ligand substitution of one Ru-coordinated CO by a dendritic phosphine termini in Reetz's 32-phosphine dendrimer under ambient conditions leading to the 32-Ru<sub>3</sub>(CO)<sub>11</sub> dendrimer-cluster.

ETC mechanism [78–80] proceeds for the introduction of the 32 cluster fragments in the dendrimer for ligation of the first Ru<sub>3</sub>(CO)<sub>11</sub> fragment to the dendritic phosphine. Then, this first complex [dendrophosphine.Ru<sub>3</sub>(CO)<sub>11</sub>] would undergo the same ETC cycle as [Ru<sub>3</sub>(CO)<sub>12</sub>] initially does to generate the bis-cluster complex {dendrophosphine.[Ru<sub>3</sub>(CO)<sub>11</sub>]<sub>2</sub>}, and so on (Scheme 16).



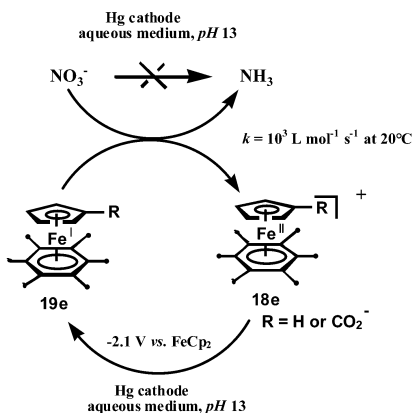
**Scheme 16** Electron-transfer-chain mechanism for the synthesis of the 96-Ru dendrimer-cluster complex.

Finally, the 64-branch phosphine DAB-*dendr*-G4-[N(CH<sub>2</sub>PPh<sub>2</sub>)<sub>2</sub>]<sub>32</sub> analogously reacts with [Ru<sub>3</sub>(CO)<sub>12</sub>] and 1 % [Fe<sup>I</sup>Cp( $\eta^6\text{-C}_6\text{Me}_6$ )] (20 °C, THF, 20 min) to give the dark-red 192-Ru dendrimer. Characterization of the purity of these dendrimer-cluster assemblies is conveniently monitored by <sup>31</sup>P NMR. This application should find extension to other metal-carbonyl clusters and other families of phosphine dendrimers.

#### WATER-SOLUBLE DENDRITIC ORGANOMETALLIC REDOX CATALYSTS: TOWARD GREEN CHEMISTRY [81]

The catalytic reduction of nitrate has been known for a long time [82], but the use of the redox catalyst [Fe<sup>II</sup>( $\eta^5\text{-C}_5\text{H}_4\text{CO}_2^-$ )( $\eta^6\text{-C}_6\text{Me}_6$ )][PF<sub>6</sub>] was the first example of an organometallic catalyst for this reaction. Electrosyntheses catalyzed by [Fe<sup>I</sup>( $\eta^5\text{-C}_5\text{H}_4\text{R}$ )( $\eta^6\text{-C}_6\text{Me}_6$ )] under these conditions showed that

$\text{NH}_3$  was produced in 63 % chemical yield and 57 % electrical yield with  $\text{R} = \text{CO}_2^-$ . Nitrite, hydroxylamine, hydrazine, and dinitrogen (minute amounts) were intermediates toward the formation of ammonia. The cathodic reduction stopped at the level of hydroxylamine when the experiment was carried out at pH 7 instead of 13. Kinetic studies in homogeneous basic aqueous solution using a polarographic method were carried out with  $[\text{Fe}^{\text{II}}(\eta^5\text{-C}_5\text{H}_4\text{R})(\eta^6\text{-arene})][\text{PF}_6]$ ,  $\text{R} = \text{CO}_2^-$ , or when only the cationic  $\text{Fe}^{\text{II}}$  form was soluble in the medium ( $\text{R} = \text{H}$ ; arene = benzene, *m*-xylene, hexamethylbenzene). These studies led to the conclusion that the rate of redox catalysis was independent of the nature of the catalyst within this series [83], but have recently been reconsidered, however, with the series of complexes  $[\text{Fe}^{\text{II}}(\eta^5\text{-C}_5\text{H}_4\text{CO}_2^-)(\eta^6\text{-arene})][\text{PF}_6]$ , arene =  $\text{C}_6\text{Me}_6-n$ ,  $n = 0$  to 6. The polarographic, cyclic voltammetry and chronoamperometry techniques were used to investigate the kinetics of the redox catalysis. The three techniques provided similar results. Thus, the rate constant of the redox catalysis can be calculated from the enhancement of the intensity of the cyclovoltammogram wave observed upon addition of the nitrate or nitrite salt into the electrochemical cell (Scheme 17). A Marcus-type linear relationship was found between the logarithms of the rate constants, and the standard redox potentials of the catalysts, indicating that the electron transfer in solution between the 19-electron  $\text{Fe}^{\text{I}}$  complex and nitrate or nitrite ion is rate-limiting [33,84].



**Scheme 17** Redox-catalysis mechanism for the cathodic reduction of nitrate (and nitrite) to  $\text{NH}_3$  catalyzed by the water-soluble  $\text{Fe}^{\text{II}}$  organometallic sandwich complex.

In order to investigate whether the mechanism proceeds by inner-sphere or outer-sphere electron transfer, other catalysts of the type  $[\text{Fe}^{\text{II}}(\eta^5\text{-C}_5\text{H}_4\text{CO}_2^-)(\eta^6\text{-arene})][\text{PF}_6]$  were synthesized with bulky arenes such as 1,3,5-tris-*t*-butylbenzene and  $\text{C}_6(\text{CH}_2\text{CH}_2\text{C}_6\text{H}_4\text{OH}-p)_6$ . In these catalysts, the redox-active group is at the center of a star- or dendritic core framework. The rate constants were found to be one to two orders of magnitude lower than what would be expected for the same driving force if the steric effect was not interfering, by comparison with the above series of catalysts with polymethylbenzene ligands. This showed a significant inner-sphere component to the electron-transfer process, although the kinetic drop would have been even more dramatic with a fully inner-sphere electron-transfer mechanism. It is likely that nitrate and nitrite ions coordinate to the 17-electron form of the  $\text{Fe}^{\text{I}}$  catalysts and that electron transfer proceeds in such intermediates rather than by outer sphere. However, the bond between an oxygen atom of nitrate or nitrite to such a low oxidation-state center must be very loose and long because  $\pi$ -back bonding is impossible with these ligands [84].

We also synthesized water-soluble hexametallic redox catalysts of this type. In the beginning of the section ‘‘Organometallic Syntheses of Polyallyl Dendritic Cores, Dendrons, and Large Dendrimers’’, we described the  $\text{CpFe}^+$ -induced hexaallylation of hexamethylbenzene, and indicated that the hexabutenylarene could be hydroborated, which led to a hexaol after oxidation, then reaction with *p*-hydroxyben-

zaldehyde gave the hexabenzaldehyde star. The hexanuclear catalyst is made by reaction of the latter with a heterobifunctional redox catalyst of the  $[\text{FeCp}(\text{arene})]^+$  type bearing an amino group on the Cp substituent for linking to a star branch and a carboxylate group on the benzene ring for solubilization in water. Thus, one may now compare the kinetics of a  $[\text{FeCp}(\text{arene})]^+$ -centered star or dendritic core to that of a star bearing  $[\text{FeCp}(\text{arene})]^+$  catalysts at the periphery. Remarkably, the kinetics of catalysts bearing the  $[\text{FeCp}(\text{arene})]^+$  moiety at the center of a star or dendritic core is one order of magnitude lower than that of such a star bearing the catalyst at the periphery. We know that, as in cytochromes, electron transfer between an electrode and a redox center located at the center of a dendrimer is slow. On the other hand, the kinetics of the hexanuclear star in which the redox moieties are located at the star periphery is about the same as those of mononuclear redox catalysts of the same type and driving force. This category of electron transfer between an electrode and redox centers located at a dendritic periphery is fast due to the fast rotation of the dendrimer as compared to the electrochemical time scale. Note that we have first chosen a star topography rather than a dendritic one in order to avoid the problem of bulk encountered in dendrimers in which the catalytic groups located on the periphery are marred by steric inhibition, preventing the substrate to approach the metal coordination sphere. By the way, this redox-catalysis technique could be very useful in order to learn more about this very problem in dendrimers. Work along this line is indeed in progress in our laboratory.

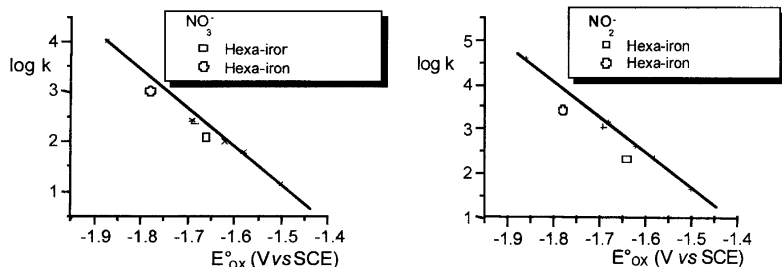


**Fig. 4** Marcus-type relationship between the kinetics ( $\ln k$ ) and thermodynamics ( $E_{1/2}$ ) for the redox-catalyzed reduction of nitrate indicating that the primary electron-transfer (mainly outer-sphere) is rate-limiting. The crosses on the lines correspond to mono-iron complexes with different driving forces, and two star hexanuclear complexes are shown for comparison.

## OUTLOOK

Dendrimers are no longer solely a nice idea, but now become better and better characterized thanks to modern techniques of nanosciences such as MALDI TOF mass spectrometry, transmission electron microscopy, and atomic force microscopy along with some classic techniques such as multi-nucleus NMR, and cyclic voltammetry [85a,86]. Yet, it was necessary to find and use powerful organometallic activation reactions such as the ones described here that usually work at room temperature quantitatively on large scales in order to provide the molecular bricks (dendritic cores and dendrons) for their construction. The resulting nanoscale metallodendritic molecules designed thereof are of multiple use in interdisciplinary areas such as catalysis (the recycling problem) [14,87,88], molecular electronics [85b,89–91] (molecular batteries, derivatized electrodes) [60], and molecular recognition (dendritic exo-receptors as sensors for anions) [92]. Molecular recognition is a key factor for biological transport and gene therapy [93]. In this sense, dendrimers behave as artificial viruses that, unlike viruses, are eventually nontoxic. Other subfields such as magnetism will shortly benefit from this approach. Dendrons can be connected to various forms of nanodevices such as stars and dendritic cores, nanoparticles, and surfaces (self-assembled monolayers), which considerably expand their potential applications. Our laboratory is now engaged in metallodendritic catalysis, nanomolecular electronic and

nanomolecular recognition (including DNA fragments), and is scrutinizing interdisciplinary applications in the spirit defined here.

### ACKNOWLEDGMENTS

I warmly thank the colleagues, students, and post-docs cited in the references who have contributed to the ideas and efforts of this research program. I am especially indebted in this respect to my close colleagues of the Université Bordeaux I, Drs. Jaime Ruiz, Sylvain Nlate (LCOO: syntheses and electrochemistry), and Sylvain Lazarre (LCPT: AFM), to Dr. Jean-Claude Blais (University Paris VI: MALDI TOF mass spectrometry) and Prof. François Varret (University of Versailles: Mössbauer spectroscopy). I am also grateful to Victor Martinez from our group for his valuable help in the preparation of the templated manuscript. Financial support from the Institut Universitaire de France (IUF), the Université Bordeaux I, the Centre National de la Recherche Scientifique (CNRS), the Alexander von Humboldt Fundation, Iberdrola, the Picasso and Erasmus-Socrates programs, the European Community, and the Region Aquitaine is gratefully acknowledged.

### REFERENCES

1. R. H. Crabtree. *The Organometallic Chemistry of the Transition Metals*, 3<sup>rd</sup> ed., Wiley, New York (2001).
2. T. M. Trnka and R. H. Grubbs. *Acc. Chem. Res.* **34**, 18 (2001) and references cited therein.
3. R. R. Schrock, J. S. Murdzek, G. C. Bazan, J. Robbins, M. DiMare, M. O'Regan. *J. Am. Chem. Soc.* **112**, 8378 (1990).
4. (a) 72 % e.e. in hydrogenation with DIOP: H. B. Kagan and T. P. Dang. French Patent 7044632 (1970) and extension to U.S. Patent 3,798,241 (1974); (b) *Chem. Commun.* 481 (1971); (c) *J. Am. Chem. Soc.* **94**, 6429 (1972).
5. See the 2001 Nobel Lectures in *Angew. Chem., Int. Ed.* (2002): (a) R. Noyori. *Angew. Chem., Int. Ed.* **41**, 2002 (2002); (b) K. B. Sharpless. *Angew. Chem., Int. Ed.* **41**, 2024 (2002); (c) W. S. Knowles. *Angew. Chem., Int. Ed.* **41**, 1998 (2002).
6. *Applied Homogeneous Catalysis with Organometallic Compounds*, B. Cornils and W. A. Herrmann (Eds.), VCH, Weinheim (1996).
7. *Handbook of Heterogeneous Catalysis*, G. Ertl, H. Knözinger, J. Weitkamp (Eds.), Wiley-VCH, Weinheim (1998).
8. *Catalysis from A to Z, A Concise Encyclopedia*, B. Cornils, W. A. Herrmann, R. Schlögl, C.-H. Wong, Wiley-VCH, Weinheim (2000).
9. For a comprehensive review, see: N. Ardoine and D. Astruc. *Bull. Soc. Chim. Fr.* **132**, 875 (1995).
10. For a recent book, see: G. R. Newkome, C. N. Moorefield, F. Vögtle, *Dendrimers and Dendrons. Concept, Syntheses, Applications*, Wiley-VCH, Weinheim (2001).
11. C. Valério, J.-L. Fillaut, J. Ruiz, J.-C. Guittard, J.-C. Blais, D. Astruc. *J. Am. Chem. Soc.* **117**, 2588 (1997).
12. C. Valério, E. Alonzo, J. Ruiz, J.-C. Blais, D. Astruc. *Angew. Chem., Int. Ed.* **38**, 1747 (1999).
13. (a) A. Labande, J. Ruiz, D. Astruc. *J. Am. Chem. Soc.* **124**, 1782 (2002); (b) A. Labande and D. Astruc. *Chem. Commun.* 1007 (2000).
14. E. Alonso, A. Labande, L. Raehm, J.-M. Kern, D. Astruc. *C. R. Acad. Sci. Ser. IIc* **2**, 209 (1999).
15. (a) H. Trujillo, C. Casado, J. Ruiz, D. Astruc. *J. Am. Chem. Soc.* **121**, 5674 (1999); (b) D. Astruc. *Acc. Chem. Res.* **33**, 287 (2000).
16. C. C. Lee, B. R. Steele, K. J. Demchuk, R. G. Sutherland. *Can. J. Chem.* **57**, 946 (1979).
17. For the synthesis of  $[\text{Fe}^{\text{II}}\text{Cp}(\eta^6\text{-C}_6\text{Me}_6)][\text{PF}_6]$ , see references 18, 19, and 35.
18. P. L. Pauson and W. E. Watts. *J. Chem. Soc.* 2990 (1963).

19. D. Astruc, J.-R. Hamon, M. Lacoste, M.-H. Desbois, E. Román. *Organometallic Synthesis*, R. B. King (Ed.), Vol. IV, p. 172 (1988).
20. J.-R. Hamon, J.-Y. Saillard, A. Le Beuze, M. McGlinchey, D. Astruc. *J. Am. Chem. Soc.* **104**, 3755 (1982).
21. F. Moulines and D. Astruc. *Angew. Chem., Int. Ed. Engl.* **27**, 1347 (1988).
22. F. Moulines and D. Astruc. *Chem. Commun.* 614 (1989).
23. For another elegant route to hexaalkylarenes, see: B. R. Steele and C. G. Scettas. *J. Am. Chem. Soc.* **122**, 2391 (2000).
24. (a) J.-L. Fillaut, J. Linares, D. Astruc. *Angew. Chem., Int. Ed. Engl.* **33**, 2460 (1994); (b) J.-L. Fillaut, R. Boese, D. Astruc. *Synlett* 55 (1992); (c) J.-L. Fillaut and D. Astruc. *New J. Chem.* **20**, 945 (1996).
25. B. Alonso, J.-C. Blais, D. Astruc. *Organometallics* **21**, 1001 (2000).
26. F. Moulines, B. Gloaguen, D. Astruc. *Angew. Chem., Int. Ed. Engl.* **28**, 458 (1992).
27. H. W. Marx, F. Moulines, T. Wagner, D. Astruc. *Angew. Chem., Int. Ed. Engl.* **35**, 1701 (1996).
28. J. Ruiz, E. Alonso, J. Guittard, J.-C. Blais, D. Astruc. *J. Organomet. Chem.* **582** (1), 139 (1999). Issue dedicated to Alan H. Cowley.
29. F. Moulines, L. Djakovitch, J.-L. Fillaut, D. Astruc. *Synlett* 57 (1992).
30. F. Moulines, L. Djakovitch, R. Boese, B. Gloaguen, W. Thiel, J.-L. Fillaut, M.-H. Delville, D. Astruc. *Angew. Chem., Int. Ed. Engl.* **105**, 1132 (1993).
31. V. Marvaud and D. Astruc. *Chem. Commun.* 773 (1997).
32. V. Marvaud and D. Astruc. *New J. Chem.* **21**, 1309 (1997).
33. S. Rigaut, M.-H. Delville, D. Astruc. *J. Am. Chem. Soc.* **119**, 1132 (1997).
34. S. Rigaut, M.-H. Delville, J. Losada, D. Astruc. *Inorg. Chim. Acta* **334**, 225 (2002).
35. D. Astruc In *Electron Transfer in Chemistry*, V. Balzani, J. Matay, D. Astruc (Eds.), Vol. II, pp. 714–803, Wiley, Weinheim (2001).
36. C. Valério, F. Moulines, J. Ruiz, J.-C. Blais, D. Astruc. *J. Org. Chem.* **65**, 1996 (2000).
37. B. Gloaguen and D. Astruc. *J. Am. Chem. Soc.* **112**, 4607 (1990).
38. D. Buchholz, B. Gloaguen, J.-L. Fillaut, M. Cotrait, D. Astruc. *Chem. Eur. J.* **1**, 374 (1995).
39. D. Buchholz and D. Astruc. *Angew. Chem., Int. Ed. Engl.* **33**, 1637 (1994).
40. S. Marcen, S. Jimenez, M. V. Dobrinovitch, F. Lahoz, L. Oro, J. Ruiz, D. Astruc. *Organometallics* **21**, 326 (2002).
41. V. Martinez, J.-C. Blais, D. Astruc. *Org. Lett.* **4**, 651 (2002).
42. F. Moulines, L. Djakovitch, M.-H. Delville, F. Robert, P. Gouzerh, D. Astruc. *Chem. Commun.* 463 (1995).
43. F. Moulines, L. Djakovitch, D. Astruc. *New J. Chem.* **20**, 1071 (1996).
44. (a) V. Sartor, L. Djakovitch, J.-L. Fillaut, F. Moulines, F. Neveu, V. Marvaud, J. Guittard, J.-C. Blais, D. Astruc. *J. Am. Chem. Soc.* **121**, 2929 (1999); (b) V. Sartor, S. Nlate, J.-L. Fillaut, F. Djakovitch, F. Moulines, V. Marvaud, F. Neveu, J.-C. Blais. *New J. Chem.* **24**, 351 (2000).
45. S. Nlate, Y. Neto, J.-C. Blais, J. Ruiz, D. Astruc. *Chemistry Eur. J.* **8**, 171 (2002).
46. S. Nlate, J. Ruiz, D. Astruc. *Chem. Commun.* 417 (2000).
47. S. Nlate, J. Ruiz, V. Sartor, R. Navarro, J.-C. Blais, D. Astruc. *Chem. Eur. J.* **6**, 2544 (2000).
48. B. Marciniec. In *Applied Homogeneous Catalysis with Organometallic Compounds*, B. Cornils and W. A. Herrmann, (Eds.), Vol. 1, Chap. 2.6, VCH, Weinheim (1996).
49. L. N. Lewis, J. Stein, K. A. Smith. In *Progress in Organosilicon Chemistry*, B. Marciniec and J. Chojnowski, (Eds.), p. 263, Gordon and Breach, Langhorne, USA (1995).
50. K. H. Pannell and H. Sharma. *Organometallics* **10**, 954 (1991).
51. P. Jutzi, C. Batz, B. Neumann, H. G. Stammmer. *Angew. Chem., Int. Engl.* **35**, 2118 (1996).
52. J. B. Flanagan, S. Margel, A. J. Bard, F. C. Anson. *J. Am. Chem. Soc.* **100**, 4248 (1978).

53. (a) D. Astruc, C. Valério, J.-L. Fillaut, J.-R. Hamon, F. Varret. In *Magnetism, "A Supramolecular Function"*, O. Kahn, (Ed.), p. 1107, NATO ASAI Series, Kluver, Dordrecht (1996); (b) C. Valério, PhD Thesis, Université Bordeaux I (1996).
54. (a) I. Cuadrado, M. Morán, C. M. Casado, B. Alonso, F. Lobete, B. Garcia, J. Losada. *Organometallics* **15**, 5278 (1996); (b) K. Takada, D. J. Diaz, H. Abruña, I. Cuadrado, C. M. Casado, B. Alonso, M. Morán, J. Losada. *J. Am. Chem. Soc.* **119**, 10763 (1997).
55. Reviews: (a) C. M. Casado, I. Cuadrado, M. Moran, B. Alonso, B. Garcia, B. Gonzales, J. Losada *Coord. Chem. Rev.* **185–6**, 53 (1999); (b) I. Cuadrado, M. Moran, C. M. Casado, B. Alonso, J. J. Losada. *Coord. Chem. Rev.* **189**, 123 (1999); (c) M. A. Hershaw and J. R. Moss. *Chem. Commun.* 1 (1999); (d) G. R. Newkome, E. He, C. N. Moorefield. *Chem. Rev.* **99**, 1689 (1999).
56. J. Ruiz and D. Astruc. *C. R. Acad. Sci. Paris, t. I, Série II c* 21 (1998).
57. R. L. Collins. *J. Chem. Phys.* **42**, 1072 (1965).
58. S. J. Green, J. J. Pietron, J. J. Stokes, M. J. Hostetler, H. Vu, W. P. Wuelfing, R. W. Murray. *Langmuir* **14**, 5612 (1998).
59. C. B. Gorman, J. C. Smith, M. W. Hager, B. L. Parhurst, H. Sierzputowska-Gracz, C. A. Haney. *J. Am. Chem. Soc.* **121**, 9958 (1999).
60. R. Murray In *Molecular Design of Electrode Surfaces*, R. Murray (Ed.,) p. 1, Wiley, New York (1992).
61. P. J. Dandliker, F. Diederich, M. Gross, B. Knobler, A. Louati, E. M. Stanford. *Angew. Chem., Int. Ed. Engl.* **33**, 1739 (1994).
62. G. R. Newkome, R. Güther, C. N. Moorefield, F. Cardullo, L. Echegoyen, F. Pérez-Cordero, H. Luftmann. *Angew. Chem., Int. Ed. Engl.* **34**, 2023 (1995).
63. H.-F. Chow, I. Y.-K. Chan, D. T. W. Chan, R. W. M. Kwok. *Chem. Eur. J.* **2**, 1085 (1996).
64. P. J. Dandliker, F. Diederich, H.-F. Chow, I. Y.-K. Chan, R. W. M. Kwok. *Chem. Eur. J.* **2**, 10859 (1996).
65. J. Issberner, F. Vögtle, L. De Cola, V. Balzani. *Chem. Eur. J.* **3**, 706 (1997).
66. C. B. Gorman, B. L. Parkhurst, W. Y. Su, K. Y. Chen. *J. Am. Chem. Soc.* **119**, 1141 (1997).
67. D. K. Smith and F. Diederich. *Chem. Eur. J.* **4**, 2353 (1998).
68. J. Ruiz, F. Ogliaro, J.-Y. Saillard, J.-F. Halet, F. Varret, D. Astruc. *J. Am. Chem. Soc.* **120**, 11693 (1998).
69. M. V. Rajasekharan, S. Giesynski, J. H. Ammeter, N. Oswald, J.-R. Hamon, P. Michaud, D. Astruc. *J. Am. Chem. Soc.* **104**, 129 (1982).
70. D. Astruc, J.-R. Hamon, G. Althoff, E. Roman, P. Batail, P. Michaud, J.-P. Mariot, F. Varret, D. Cozak. *J. Am. Chem. Soc.* **101**, 5445 (1979). This paper also reports the first CpFe<sup>+</sup>-induced iterative starburst hexaalkylation of C<sub>6</sub>Me<sub>6</sub>.
71. J.-R. Hamon, D. Astruc, P. Michaud. *J. Am. Chem. Soc.* **103**, 7589 (1981).
72. J. Ruiz, C. Pradet, F. Varret, D. Astruc. *Chem. Commun.* 1108 (2002).
73. C. Bossard, S. Rigaut, D. Astruc, M.-H. Delville, G. Félix, A. Février-Bouvier, J. Amiell, S. Flandrois, P. Delhaès. *Chem. Commun.* 333 (1993).
74. Redox potentials of the six cathodic monoelectronic reductions of C<sub>60</sub>: A. Xie, E. Pérez-Cordero, L. Echegoyen. *J. Am. Chem. Soc.* **114**, 3978 (1992).
75. E. Alonso and D. Astruc. *J. Am. Chem. Soc.* **122**, 3222 (2000).
76. (a) M. I. Bruce, D. C. Kehoe, J. G. Mattisons, B. K. Nicholson, P. H. Rieger, M. L. J. Williams. *Chem. Commun.* 442 (1982); (b) M. I. Bruce, J. G. Mattisons, B. K. Nicholson. *J. Organomet. Chem.* **247**, 321 (1983).
77. (a) M. T. Reetz, G. Lohmer, R. Scwickardi. *Angew. Chem., Int. Ed. Engl.* **36**, 1526 (1997). This article reports several typical examples of the use of dendritic phosphines in catalysis; (b) E. M. M. de Brabander-van den Berg and E. W. Meijers. *Angew. Chem., Int. Ed. Engl.* **32**, 1308 (1993).

78. First example of recognized ETC-catalysis. R. Rich and H. Taube. *J. Am. Chem. Soc.* **76**, 2608 (1954).
79. Comprehensive review on ETC catalyzed reactions. D. Astruc. *Angew. Chem., Int. Ed. Engl.* **27**, 643 (1988). See also ref. 80.
80. (a) D. Astruc. *Electron Transfer and Radical Processes in Transition-Metal Chemistry*, VCH, New York (1995); (b) IBID, Chap. 6, “Chain Reactions”, pp. 413–478.
81. *Green Chemistry*, P. T. Anastas and T. C. Williamson (Eds.), ACS Symp. Ser. 626, American Chemical Society, Washington, DC (1996).
82. M. Tokuaka. *Collect. Czech. Chem. Commun.* **4**, 444 (1932); **6**, 339 (1934).
83. A. Buet, A. Darchen, C. Moinet. *Chem. Commun.* 447 (1979).
84. S. Rigaut, M.-H. Delville, J. Losada, D. Astruc. *Inorg. Chim. Acta* **334**, 225 (2000). Issue dedicated to Andrew Wojcicki.
85. A. E. Kaifer and M. Gomez-Kaifer. *Supramolecular Electrochemistry*, Wiley-VCH, Weinheim (1999).
86. *Electron Transfer and Radical Processes in Transition-Metal Chemistry*, (a) Chap. 2: “Electrochemistry”, pp. 89–195; (b) Chap. 4: “Molecular Electronics”, pp. 283–322.
87. G. E. Oosterom, J. N. H. Reek, P. C. J. Kamer, P. W. N. M. van Leeuwen. *Angew. Chem., Int. Ed.* **40**, 1828 (2001).
88. R. Kreiter, A. W. Kleij, R. J. Klein Gebbink, G. van Koten. In *Dendrimer IV: Metal Coordination, Self Assembly, Catalysis*, F. Vögtle and C. A. Schalley (Eds.), *Top. Curr. Chem.*, Springer Verlag, Berlin **217**, 163 (2001).
89. M. Mayor, M. Buschel, K. M. From, J.-M. Lehn, J. Daub. *Ann. N.Y. Acad. Sci.* **960**, 16 (2002).
90. J. M. Reimers, W. A. Shapley, N. Lambropoulos, N. S. Hush. *Ann. N.Y. Acad. Sci.* **960**, 100 (2002).
91. J. Chen, W. Wang, J. Klemic, M. A. Reed, B. W. Axelrod, D. M. Kascak, A. M. Rawlett, D. W. Price, S. M. Dirk, J. M. Tour. *Ann. N.Y. Acad. Sci.* **960**, 69 (2002)
92. P. D. Beer and P. A. Gale. *Angew. Chem., Int. Ed.* **40**, 486 (2001).
93. For a review on dendrimers in molecular biology, see: D. Astruc. *C. R. Acad. Sci. Paris I* 322, *Série IIb* 757 (1996).